Progress In Electromagnetics Research, PIER 80, 321–336, 2008

PREDICTION OF THE SAR LEVEL INDUCED IN A DIELECTRIC SPHERE BY A THIN WIRE DIPOLE ANTENNA

N. K. Kouveliotis and C. N. Capsalis

National Technical University of Athens
School of Electrical and Computer Engineering
Division of Information Transmission Systems
and Material Technology
9, Iroon Polytechniou Str., Zografou 157 73, Athens, Greece

Abstract—The interaction between a dipole antenna, representing a simplified model of a mobile terminal, and a homogeneous spherical model of the human head is examined. The Finite Difference Time Domain (FDTD) method is utilized, to calculate the either peak or average value of the Specific Absorption Rate (SAR), corresponding to different distances between antenna and phantom. The variation of the SAR with the distance between the mobile antenna and the human phantom has gained significant attention in the recent literature and is investigated here. An attempt to correlate the computed SAR values with the basic antenna characteristics, such as the standing wave ratio (SWR), reveals that a precise estimation of the level of the SAR can be achieved regarding data acquired from the mobile terminal.

1. INTRODUCTION

The recent widespread use of portable and mobile radio transmitters has excited the investigation of the impact of the mobile antenna on the human body, as well as the degradation of the antenna's performance due to the presence of such a biological scatterer. This investigation has been implemented through many ways, such as the computation or measurement of the level of the peak or average over 1 g or 10 g Specific Absorption Rate (SAR) induced in the human body [1–5]. Moreover, the variation of the antenna's input impedance, radiation efficiency and radiation patterns has also been extensively studied [6–14] involving various types of antennas, human phantoms and arithmetic techniques or experimental configurations. However, the complexity of the mobile

antenna combined with the more complicated and unique structure of each human body, have prevented the extraction of a generic and safe conclusion involving this specific interaction.

The need to predict the SAR level induced in the human body with regard to the distance or to other antenna parameters has also been treated in the literature. An approximation formula presented in [15], provides an estimation of the spatial peak SAR depending on the incident H-field or the current on the antenna and on the conductivity and permittivity of the human tissue. This formula was derived by numerical computations and experimental results with the use of a half-wavelength dipole antenna placed parallel to a plane phantom filled with tissue simulating liquid. The spatial peak SAR can be computed through the proposed formula with respect to different distances between antenna and phantom, with an uncertainty of 3 dB and can be generalized for spheres with large diameters and heterogeneous bodies. An analytical form of the rectangular components of the electromagnetic field induced in a two-layer plane phantom, as a function of the distance, is introduced in [16]. The source antenna is represented by a dipole close and parallel to one side of the head and the amplitude and distribution of the dipole's current is used to determine the amplitude of the induced field in the phantom. Additional results presented in [17], approximate in a high degree the formula proposed in [15] and are in agreement with [16], for a half-wavelength dipole antenna positioned near a uniform semi-infinite plane, a uniform sphere and a uniform or realistic head model. The dipole antenna is often used in simulation studies due to the smaller simulation space that it occupies and the fact that it can give a conservative estimation of the SAR induced by a monopole antenna [18].

The variation of the SAR with the distance between the mobile antenna and the human phantom is as well investigated in some additional studies. A quarter-wavelength monopole positioned on a metal box representing a generic mobile terminal, interacting with a head model simulated as a set of Magnetic Resonance Imaging (MRI) slices, was modeled with the Finite Difference Time Domain (FDTD) method [18]. SAR values were computed for different separations between antenna and head as well as with and without the presence of the user's hand. The replacement of the monopole handset with a dipole antenna reveals that higher values of SAR are obtained. Similar results were derived with the same method in [19]. Moreover, in [20, 21] the use of different configurations of the human head coupled to a dipole antenna, pointed out that the average spatial peak SAR values are slightly dependent on the shape, size or whether the phantom is homogeneous or not. The homogeneous representation of the human

phantom is proposed in these studies, as it reduces the number of tests (due to the symmetry of the antenna that is observed at the direction parallel to the surface), without simultaneously overestimating the average spatial peak SAR values. In [22], experimental results were acquired from a structure containing a sphere of simulated brain tissue interacting with a half-wave dipole antenna. Useful conclusions were derived concerning the variation of the SAR or the dipole's input impedance with respect to the position of the antenna in relation to the phantom or the depth inside the simulated brain tissue. A FDTD simulation [23] of a dipole antenna closely coupled to a rectangular box, constructed by multiple dielectric layers representing the different tissue types of the human head, depicted the variation of the SAR and the induced current with the distance between dipole and head. Finally in [24], a theoretical study (based on the method of moments) and an experimental verification is presented, regarding the variation of the SAR over the whole human body illuminated by a dipole antenna.

In this paper, the interaction of a dipole antenna with a homogeneous sphere filled with human tissue equivalent dielectric material is investigated. The use of the dipole antenna is strongly motivated by the fact that it provides an accurate representation of the field values induced in the human head by a mobile terminal, utilizing a simple structure and consequently avoiding any secondary effects. With the application of the FDTD method [25–32], the spatial peak SAR induced in the sphere is computed as well as the peak average SAR value over 1 g and 10 g of tissue. The input impedance is simultaneously calculated at different positions of the antenna with respect to the phantom. With the use of regression and correlation theory [33], a least-squares fit is applied to the simulation results providing an accurate prediction of the level of the SAR (peak or average) based on the distance between dipole and sphere or the standing wave ratio (SWR) on the antenna feedpoint. The simulation occurred for two different frequencies at 905 MHz and 1790 MHz which are at the modern mobile terminals' frequency region.

2. PROBLEM FORMULATION

The structure under study is shown in Figure 1.

It consists of a homogeneous sphere filled with a human tissue simulating material and of a thin wire dipole antenna placed at different distances d with respect to the phantom. The diameter of the sphere was chosen to be 20 cm which is typical for an average shape of the human head and the length of the dipole was chosen so as to achieve an adequate level of matching. Thus, at the frequency of 905 MHz

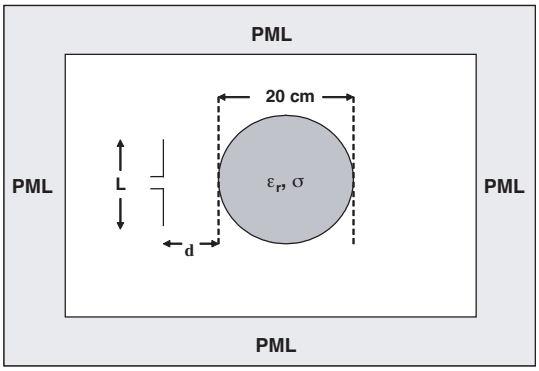

Figure 1. Structure under study.

a $L = 15.3\,\text{cm}$ dipole was used, where a length of $L = 7.5\,\text{cm}$ was satisfactory for the frequency of 1790 MHz. The excitation of the fields was provided by applying a sinusoidal voltage $V_s(t)$ of the following form at the dipole's gap:

$$V_s(t) = V_0 \sin(2\pi f_s t) \tag{1}$$

where V_0 is the magnitude of the applied voltage and f_s is the frequency of propagation.

The dielectric material used to simulate the human head, was chosen so as its relative permittivity ε_r and conductivity σ were in accordance with the EN 50383 standard [34]. In Table 1, the values of ε_r and σ for each examined frequency are shown. The density of the simulated tissue was set at $\rho = 1000\,\text{kg/m}^3$.

Table 1. Values of ε_r and σ of the human tissue simulating material contained in the homogeneous sphere, for each frequency of interest.

	905 MHz	**1790 MHz**
ε_r	42.29	40.07
σ	0.996	1.37

The FDTD method was employed to compute the field values at each position of interest. The spatial segment used for the application of the method was chosen to be equal in the three dimensions and

had a value of $\Delta x = 3\,\text{mm}$, so as to combine an acceptable level of convergence in the simulation results with a tolerable time of implementation regarding the available computer resources. According to FDTD principles or the Courant criterion [25], the time step was chosen to be $\Delta t = 0.5 \cdot 10^{-11}\,\text{sec}$. The simulation occurred for approximately 20 periods of the applied sinusoidal voltage after which a fine steady state situation was observed. The thin wire dipole antenna was implemented through the FDTD method by setting the parallel to the dipole axis electric field component (E_z for this study) equal to zero across the dipole's length, except for the gap where the voltage described in Equation (1) was applied. The gap had a width of one spatial step (i.e., 3 mm). In order to achieve free space conditions, a generalized perfectly matched layer (GPML) described in [35] is applied, which extends the conventional PML [25] to absorb both propagating and evanescent waves. The width of the PML was 15 layers and it was found adequate for the examination of FDTD problems of this type concerning convergence issues.

3. SIMULATION RESULTS

At the beginning of the simulation procedure, the antenna characteristics in the free space environment (i.e., without the presence of the human head phantom) were determined. Thus, the antenna input impedance at the two examined frequencies was derived through the calculation of the current I_s at the dipole's gap, which was performed with the following equation:

$$I_s(t) = \left(H_x^{n+1/2}(i,j-1,k)\right) - H_x^{n+1/2}(i,j,k) + H_y^{n+1/2}(i,j,k) - H_y^{n+1/2}(i-1,j,k)) \cdot \Delta x \quad (2)$$

where H_x, H_y are the x, y components respectively of the magnetic field, i, j, k represent the indexes for each spatial segment at the x, y, z direction respectively, and n stands for the temporal step index. This equation is produced by the discretization of the Ampere's contour law around the gap [25].

The length of the dipole at the two frequencies was adjusted so as to achieve a satisfying level of matching. So, at the frequency of 905 MHz, a 15.3 cm dipole gave an input impedance of $Z_{in}^{freespace} = 71.46 - j2.03\,\Omega$, where at the frequency of 1790 MHz, a 7.5 cm dipole gave an input impedance of $Z_{in}^{freespace} = 71.5\,\Omega$.

The presence of the biological scatterer in the close vicinity of the dipole, brings on a significant alteration in the driving point input impedance of the antenna. The values of the input impedance Z_{in}

for each simulated frequency with respect to the distance between the dipole and the outer surface of the human head phantom are shown in Table 2.

Table 2. Results of the dipole's input impedance and the magnitude of the corresponding correlation coefficient with respect to distance d and at each frequency of interest

	905 MHz		**1790 MHz**	
d **(m)**	$Z_{in}(\Omega)$	$\lvert\rho\rvert$	$Z_{in}(\Omega)$	$\lvert\rho\rvert$
0.009	45.04 - j22.03	0.279	37.38 - j4.22	0.316
0.012	43.19 - j16.73	0.274	38.06 + j2.14	0.306
0.015	42.21 - j12.34	0.271	40.52 + j9.27	0.288
0.018	41.80 - j9.67	0.269	44.73 + j12.92	0.254
0.021	42.39 - j6.07	0.257	49.15 + j17.24	0.232
0.024	43.45 - j2.47	0.244	54.33 + j19.07	0.202
0.027	44.78 + j1.27	0.231	59.16 + j20.75	0.182
0.030	46.42 + j2.64	0.216	63.54 + j22.29	0.173
0.033	48.27 + j4.13	0.200	68.58 + j19.80	0.142
0.036	50.26 + j5.74	0.185	71.86 + j20.75	0.143
0.039	52.06 + j8.97	0.180	75.63 + j17.30	0.120
0.042	54.30 + j9.35	0.164	78.55 + j13.38	0.100
0.045	56.48 + j9.73	0.149	80.72 + j9.12	0.085
0.048	58.31 + j11.76	0.146	81.58 + j9.21	0.089
0.051	60.36 + j12.17	0.136	82.31 + j4.63	0.076

The distance was assumed to be varied between 0.9 cm and 5.1 cm, which is the actual distance range between the mobile terminal and the human head due to the presence of the human ear and the different structural attributes of the modern mobile devices. In the same table, the magnitude of the corresponding correlation coefficient ρ for the different positions of the antenna with respect to the phantom and for the two frequencies of interest, is depicted. The correlation coefficient is calculated using the following equation:

$$\rho = \frac{Z_{in} - Z_{in}^{free\ space}}{Z_{in} + Z_{in}^{free\ space}} \tag{3}$$

As it is observed from Table 2, a significant degradation in the dipole's input impedance with regard to the free space results is indeed perceived for each frequency and it is due to the presence of the dielectric sphere. Accordingly, the magnitude of the correlation coefficient is being decreased with the increment in the separation distance between the dipole and phantom in order to converge to the free space conditions where the coupling between the dipole and sphere is eliminated. This decrement appears to be more rapid at the frequency of 1790 MHz and this is absolutely prospective considering the smaller (in relation to 905 MHz) wavelength.

The value of the SAR at each position inside the phantom was determined according to Equation (4), by computing the magnitude $|E_t|$ of the total electric field via the FDTD method:

$$SAR = \frac{\sigma |E_t|^2}{2\rho} \tag{4}$$

Then, the spatial peak SAR value was recorded as well as the peak average SAR value over 1 g or 10 g of tissue. The results of each SAR distribution with respect to the distance between dipole and sphere at each examined frequency are shown in Figures 2 and 3. Each SAR value was normalized to the antenna radiated power at every examined position.

In the same Figures, an approximation formula that best fits the variation of the SAR with distance d was also evaluated with the least-squares method used in regression theory [33]. The correlation coefficient r, used to determine the correlation between the regression curve and the sample points is expressed in Equation (5) [33].

$$r^2 = \frac{\sum_{i=1}^{N} (y_{i,est} - \bar{y})^2}{\sum_{i=1}^{N} (y_i - \bar{y})^2} \tag{5}$$

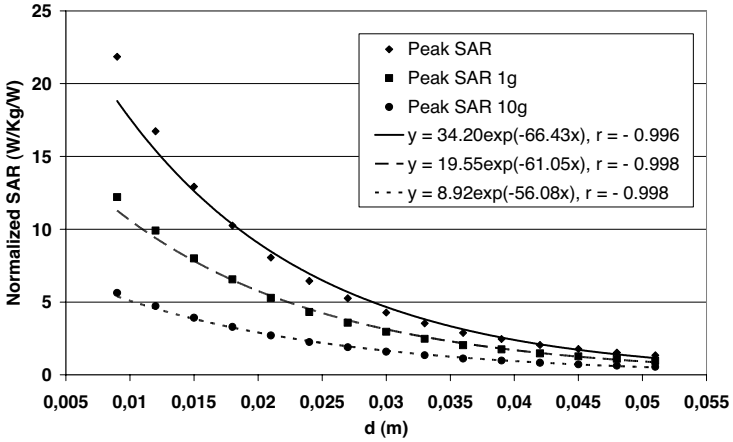

Figure 2. Variation of normalized spatial peak SAR, peak average SAR over 1 g and peak average SAR over 10 g with respect to the distance d between dipole and sphere at the frequency of 905 MHz and the corresponding regression curves.

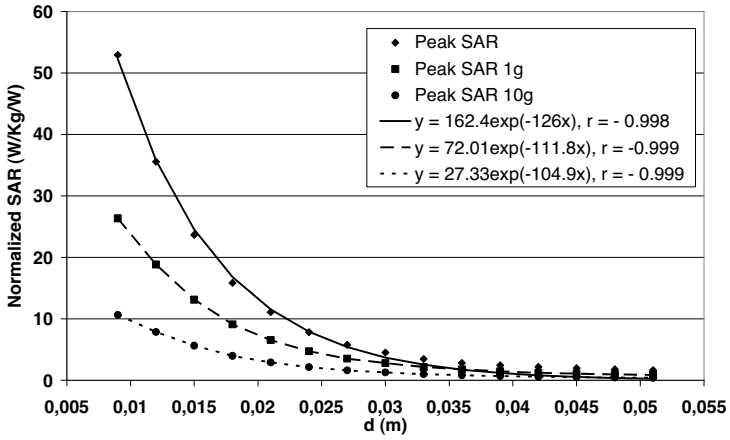

Figure 3. Variation of normalized spatial peak SAR, peak average SAR over 1 g and peak average SAR over 10 g with respect to the distance d between dipole and sphere at the frequency of 1790 MHz and the corresponding regression curves.

where for a sample point (x_i, y_i), $y_{i,est}$ is the estimated value from the regression curve of the y coordinate of x_i, $\bar{y}$ corresponds to the mean value of the $y_{i,est}$ values and N is the number of samples.

The value of r appears to approach unity for every proposed regression curve, as it can be drawn out from Figures 2 and 3, leading to the conclusion that the proposed exponential formulas best fit the numerical results and consequently, an accurate estimation of the peak SAR or peak average SAR can be determined. The exponential variation of the SAR with the distance, already derived in the literature [18, 22], reinforces the stability of the developed FDTD code combined with the applied fitting procedure.

In Figures 4 and 5, the results derived with the application of the approximation formula suggested in [15], using the generalized multipole technique (GMT) are depicted, providing a verification of the calculated spatial peak SAR values. The slight differences that are observed are attributed to the smaller length (about 0.45λ) of the dipole antenna used in our study, compared to the half-wavelength dipole that is anticipated in [15] and are within the limit of 3 dB indicated in the late study. Moreover, the difference between the two antenna lengths provides an indication of independence, under limits of uncertainty, of the results regarding the dipole length.

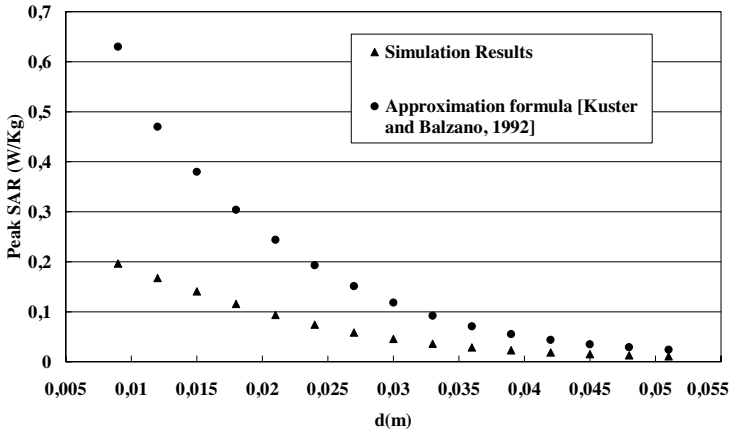

Figure 4. Comparison between simulated spatial peak SAR values and calculated SAR values derived from approximation formula presented in [15] at the frequency of 905 MHz.

Following the same procedure, the SAR values (spatial peak or peak averaged over 1 g or 10 g) were correlated with the SWR on the antenna feed point, for each position of the antenna in relation to the phantom, by utilizing the results demonstrated in Table 2. Figures 6 and 7 show the variation of the SAR with SWR and the corresponding regression curves for each examined frequency. Similar

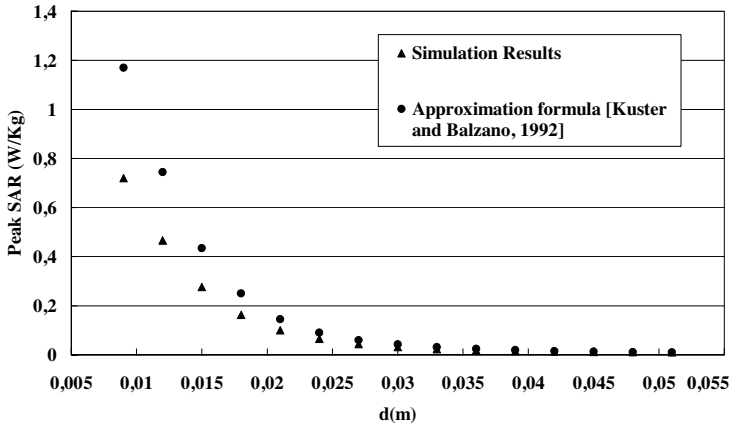

Figure 5. Comparison between simulated spatial peak SAR values and calculated SAR values derived from approximation formula presented in [15] at the frequency of 1790 MHz.

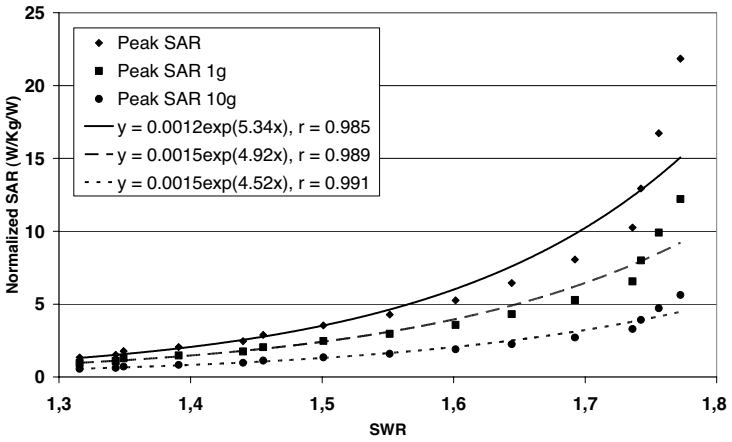

Figure 6. Variation of normalized spatial peak SAR, peak average SAR over 1 g and peak average SAR over 10 g with respect to the SWR on the dipole's feed point, at different positions of the antenna with respect to the phantom, at the frequency of 905 MHz and the corresponding regression curves.

to the previous correlation outcome, the r values for every case under study are very close to 1, providing adequate approximation formulas for the prediction of the SAR level with regard to the fundamental antenna characteristics (i.e., input impedance).

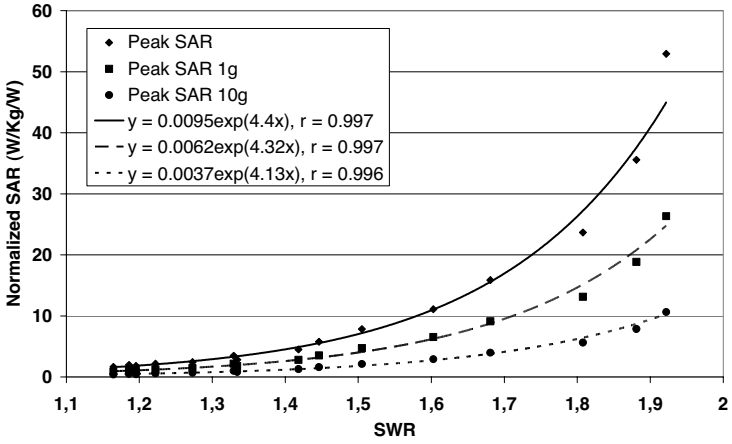

Figure 7. Variation of normalized spatial peak SAR, peak average SAR over 1 g and peak average SAR over 10 g with respect to the SWR on the dipole's feed point, at different positions of the antenna with respect to the phantom, at the frequency of 1790 MHz and the corresponding regression curves.

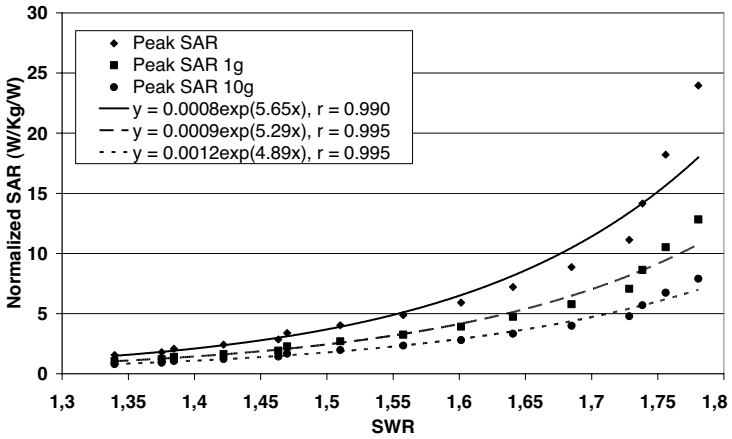

Figure 8. Variation of normalized spatial peak SAR, peak average SAR over 1 g and peak average SAR over 10 g with respect to the SWR on the dipole's feed point at different positions of the antenna with respect to the phantom, at the frequency of 905 MHz, for a sphere with radius 18 cm and the corresponding regression curves.

In order to examine the applicability of the proposed method for different configurations of the antenna-head model, two additional sphere structures consisting of the same tissue characteristics and diameters of 18 cm and 24 cm were tested. The fitting results of the correlation between the SAR and SWR at 905 MHz, are depicted in Figures 8 and 9. An exponential curve is as well derived with the proposed formulas being similar (maximum difference calculated approximately 10%) to those given for the sphere of 20 cm. Thus, the suggested method of correlation seems to be independent of the sphere diameter providing a more generalized outcome.

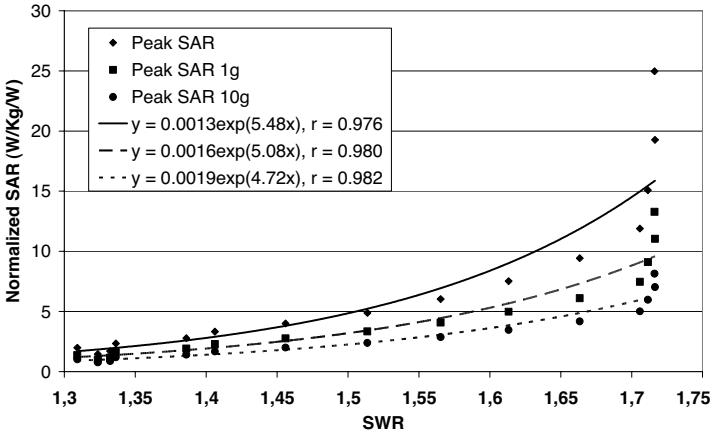

Figure 9. Variation of normalized spatial peak SAR, peak average SAR over 1 g and peak average SAR over 10 g with respect to the SWR on the dipole's feed point at different positions of the antenna with respect to the phantom, at the frequency of 905 MHz, for a sphere with radius 24 cm and the corresponding regression curves.

Moreover, considering Figures 4 and 5 where a comparison of the results of the present code with the Kuster's and Balzano's formula is given, the proposed method can be generalized to heterogeneous bodies of arbitrary shape as is implied in [15]. Different antenna structures will be simulated in the future in order to verify the absolute stability of the proposed method regarding the different antenna-head model configurations.

4. CONCLUSION

From the above demonstrated results derived from the simulation procedure, some useful remarks can be drawn out. First, the

spatial peak SAR or peak average SAR values induced in the human phantom by the thin wire dipole antenna, appear to be exponentially varied with respect to the distance between the antenna and the human head phantom. This conclusion is of great importance during the mobile terminal manufacturing, as it can provide useful information about the best position of locating the transceiver's antenna considering the stimulated health hazards. Furthermore, an exponential approximation formula was derived describing the alteration of the spatial peak SAR or peak average SAR values with the SWR at the antenna feedpoint, as the position of the dipole with respect to the human phantom is modified. Thus, the SAR level can be derived through a calculation or measurement of the antenna's input impedance. This can be practically evaluated by considering an integrated device in a mobile terminal, which by measuring the antenna's input impedance can give an accurate indication about the variation of the SAR (peak or average) induced in the human head as the transceiver is placed at different positions in relation to the head.

The findings of this paper apparently refer to the specific structure that was simulated. The need to generalize the results that were drawn out provides a strong motivation for this study to be continued. In order to ensure that the conclusions arising from such an investigation can be directly applied to modern mobile terminals, further simulations will have to be carried out, probably combined with conducted measurements, including different types of antennas and more accurate models of the human head or body. However, the results derived from the present study, supply important information (even at an elementary stage) which will enforce the simulation procedure during a higher level implementation.

ACKNOWLEDGMENT

The work of Dr. N. K. Kouveliotis is supported by the EPEAEK — Pythagoras I research program. (The project is co-funded by the European Social Fund (75%) and National Resources (25%)).

REFERENCES

1. Gandhi, O. P., G. Lazzi, and C. M. Furse, "Electromagnetic absorption in the human head and neck for mobile telephones at 835 and 1900 MHz," *IEEE Trans. Microw. Theory Techn.*, Vol. 44, No. 10, 1884–1897, 1996.
2. Watanabe, S., M. Taki, T. Nojima, and O. Fujiwara, "Characteristics of the SAR distributions in a head exposed to

electromagnetic fields radiated by a hand-held portable radio," *IEEE Trans. Microw. Theory Techn.*, Vol. 44, No. 10, 1874–1883, 1996.

3. Drossos, A., V. Santomaa, and N. Kuster, "The dependence of electromagnetic energy absorption upon human head tissue composition in the frequency range of 300–3000 MHz," *IEEE Trans. Microw. Theory Techn.*, Vol. 48, No. 11, 1988–1995, 2000.
4. Khalatbari, S., D. Sardari, A. A. Mirzaee, and H. A. Sadafi, "Calculating SAR in two models of the human head exposed to mobile phones radiations at 900 and 1800 MHz," *Progress In Electromagnetics Research Symposium*, 104–109, Cambridge, USA, March 26–29, 2006.
5. Shin, C. S., D. G. Choi, and N. Kim, "Internal monopole antenna design for multi-band operation and SAR analysis," *Progress In Electromagnetics Research Symposium*, 294–297, Hangzhou, China, August 22–26, 2005.
6. Okoniewski, M. and M. A. Stuchly, "A study of the handset antenna and human body interaction," *IEEE Trans. Microw. Theory Techn.*, Vol. 44, No. 10, 1855–1864, 1996.
7. Chuang, H. R., "Human operator coupling effects on radiation characteristics of a portable communication dipole antenna," *IEEE Trans. Antennas Propagation*, Vol. 42, No. 4, 556–560, 1994.
8. Toftgard, J., S. N. Hornsleth, and J. B. Andersen, "Effects on portable antennas of the presence of a person," *IEEE Trans. Antennas Propagation*, Vol. 41, No. 6, 739–746, 1993.
9. Lazzi, G., S. S. Pattnaik, and O. P. Gandhi, "Experimental and FDTD-computed radiation patterns of cellular telephones held in slanted operational conditions," *IEEE Trans. on Electromagn. Compatibility*, Vol. 41, No. 2, 141–144, 1999.
10. Yang, F., V. Demir, D. A. Elsherbeni, and A. Z. Elsherbeni, "Enhancement of printed dipole antennas characteristics using semi-EBG ground plane," *J. of Electromagn. Waves and Appl.*, Vol. 20, No. 8, 993–1006, 2006.
11. Ding, W., Y. Zhang, P. Y. Zhu, and C. H. Liang, "Study on electromagnetic problems involving combinations of arbitrarily oriented thin-wire antennas and inhomogeneous dielectric objects with a hybrid MOM-FDTD method," *J. of Electromagn. Waves and Appl.*, Vol. 20, No. 11, 1519–1533, 2006.
12. Kuo, L.-C., Y.-C. Kan, and H.-R. Chuang, "Analusis of a 900/1800-Mhz dual-band gap loop antenna on a handset with proximate head and hand model," *J. of Electromagn. Waves and Appl.*, Vol. 21, No. 1, 107–122, 2007.

13. Ali, M. and S. Sanyal, "A numerical investigation of finite ground planes and reflector effects on monopole antenna factor using FDTD technique," *J. of Electromagn. Waves and Appl.*, Vol. 21, No. 10, 1379–1392, 2007.
14. Sarraf, R., R. Moini, S. H. H. Sadeghi, and A. Farschtschi, "Calculation of EM characteristics of a cellular phone handset by time-domain MoM," *Progress In Electromagnetics Research Symposium*, 167–172, Prague, Czech Republic, Aug. 27–30, 2007.
15. Kuster, N. and Q. Balzano, "Energy absorption mechanism by biological bodies in the near field of dipole antennas above 300 MHz," *IEEE Trans. Vehicular Technol.*, Vol. 41, No. 1, 17–23, 1992.
16. King, R. W. P., "Electromagnetic field generated in model of human head by simplified telephone transceiver," *Radio Science*, Vol. 30, No. 1, 267–281, 1995.
17. Riu, P. J. and K. R. Foster, "Heating of tissue by near-field exposure to a dipole: A model analysis," *IEEE Trans. Biomedical Engineering*, Vol. 46, No. 8, 911–917, 1999.
18. Dimbilow, P. J. and S. W. Mann, "SAR calculations in an anatomically realistic model of the head for mobile communication transceivers at 900 MHz and 1.8 GHz," *Phys. Med. Biol.*, Vol. 39, 1537–1553, 1994.
19. Dimbilow, P. J., "FDTD calculations of the SAR for a dipole closely coupled to the head at 900 MHz and 1.9 GHz," *Phys. Med. Biol.*, Vol. 38, 361–368, 1993.
20. Hombach, V., K. Meier, M. Burkhardt, E. Kuhn, and N. Kuster, "The dependence of EM energy absorption upon human head modeling at 900 MHz," *IEEE Trans. Microw. Theory Techn.*, Vol. 44, No. 10, 1865–1873, 1996.
21. Meier, K., V. Hombach, R. Kastle, R. Y. S. Tay, and N. Kuster, "The dependence of electromagnetic energy absorption upon human head modeling at 1800 MHz," *IEEE Trans. Microw. Theory. Techn.*, Vol. 45, No. 11, 2058–2062, 1997.
22. Faraone, A., Q. Balzano, and D. Simunic, "Experimental dosimetry in a sphere of simulated brain tissue near a half-wave dipole antenna," *Proc. IEEE Int. Symp. Electromagn. Compat.*, 906–911, 1998.
23. Chen, H. Y. and H. H. Wang, "Current and SAR induced in a human head model by the electromagnetic fields irradiated from a cellular phone," *IEEE Trans. Microw. Theory Techn.*, Vol. 42, No. 12, 2249–2254, 1994.

24. Stuchly, M. A., R. J. Spiegel, S. S. Stuchly, and A. Kraszewski, "Exposure of man in the near-field of a resonant dipole: comparison between theory and measurements," *IEEE Trans. Microw. Theory Techn.*, Vol. 34, No. 1, 26–31, 1986.
25. Taflove, A., *Computational Electrodynamics: The Finite Difference Time Domain Method*, Artech House, Norwood, MA, 1995.
26. Niikura, K., R. Kokubo, K. Southisombath, H. Matsui, and T. Wakabayashi, "On analysis of planar antennas using FDTD method," *PIERS Online*, Vol. 3, No. 7, 1019–1023, 2007.
27. Gorodetsky, D. A. and P. A. Wilsey, "Reduction of FDTD simulation time with modal methods," *Progress In Electromagnetics Research Symposium*, 510–513, Cambridge, USA, March 26–29, 2006.
28. Fayedeh, H., C. Ghobadi, and J. Nourinia, "An improvement for FDTD analysis of thin-slot problems," *Progress In Electromagnetics Research B*, Vol. 2, 15–25, 2008.
29. Sha, W., X. Wu, and M. Chen, "A diagonal split-cell model for the high-order symplectic FDTD scheme," *PIERS Online*, Vol. 2, No. 6, 715–719, 2006.
30. Tang, L. and T. S. Ibrahim, "On the radio-frequency power requirements of human MRI," *PIERS Online*, Vol. 3, No. 6, 886–889, 2007.
31. Li, Y. H. and W. B. Dou, "BOR-FDTD analysis of spherical lens multi-beam antenna," *PIERS Online*, Vol. 3, No. 7, 1111–1113, 2007.
32. Chai, W., X. Zhang, and J. Liu, "A novel wideband antenna design using U-slot," *PIERS Online*, Vol. 3, No. 7, 1067–1070, 2007.
33. McPherson, G., *Statistics in Scientific Investigation*, Springer-Verlag, New York, 1990.
34. CENELEC, EN 50383: Basic standard for the calculation and measurement of electromagnetic field strength and SAR related to human exposure from radio base stations and fixed terminal stations for wireless telecommunication systems (110 MHz–40 GHz), 2002.
35. Fang, J. and Z. Wu, "Generalized perfectly matched layer for the absorption of propagating and evanescent waves in lossless and lossy media," *IEEE Trans. Microw. Theory Techn.*, Vol. 44, No. 12, 2216–2222, 1996.